

σ_z -dependent correlations with other correlation mechanisms in liquid ^3He

F. Arias de Saavedra and E. Buendía

Departamento de Física Moderna, Universidad de Granada, E-18071 Granada, Spain

(Received 20 February 1992; revised manuscript received 26 May 1992)

The role played by the correlations depending on the third component of spin, σ_z -dependent correlations, in the description of the ground state of liquid ^3He is studied. With this aim, the competition among this kind of correlations and central three-body and backflow correlations has been analyzed. This has been done using a generalization of Fermi hypernetted chain equations. Special attention has been paid to the approximation of the elementary diagrams using the two most efficient approximations: the scaling and the interpolating equation. The obtained results for the energy with both approximations are similar for all the cases studied. The increment of the energy supplied by σ_z -dependent correlations is not modified by the inclusion of three-body correlations. However, this increment disappears when backflow correlations are introduced because of a strong competition between both mechanisms of correlation.

I. INTRODUCTION

The theoretical description of the ground state of liquid ^3He has been studied using all methods developed for the treatment of strongly interacting many-body systems. Among all the results, those obtained using the Green's-function Monte Carlo (GFMC) method must be emphasized because they are close to the exact ones.¹ However, this procedure does not provide direct information about the different mechanisms that determine the dynamics of the system.

The generalization of Jastrow trial wave functions within the variational approach is an option to the previous calculations with very acceptable results. This method has allowed us to establish that for an adequate description of the ground state it must be included in the wave-function central two- and three-body correlations,² backflow,³ and full-spin correlations.⁴ The inclusion of all these correlations leads to a good agreement with the experimental results.⁴

The most important difficulty in using these trial wave functions in the variational approach is the calculation of the expectation values of the operators. Two basic techniques are used nowadays for these calculations. The first one, usually known as the variational Monte Carlo (VMC) method, is based on methods of statistical sampling of these expectation values, and it supplies the exact result of the expectation value with a statistical error intrinsic to the method. The second one uses the Fermi hypernetted chain (FHNC) equations.⁵ This last method is based on a power expansion of the expectation value in terms of some short-range functions directly related to the correlation functions. After a classification of the infinite addends, they are regrouped, generating a set of coupled integral equations that can be numerically solved. In order to do it accurately, it is necessary to approximate to the so-called elementary diagrams. There are two main techniques for getting this: the scaling^{6,3} and the interpolating equation approximations.^{7,8} Both are based on making consistent some quantities that may

be evaluated in two different ways.

The results from practical calculations where FHNC and VMC can be applied without important simplifications, i.e., for central two- and three-body correlations, are almost the same. This agreement is maintained for trial wave functions, including correlations dependent on the third component of spin and two-body central correlations.^{9,10} We must also say that the agreement is reasonable when the correlations have more complex structure as backflow correlations,^{11,3,4} although the differences are more important in these cases. Because of the noncommutation of the correlations functions with one common particle, there are no VMC calculations for full-spin correlations, which allow one to value the accuracy of the FHNC-single-operator-chain (SOC) approximation used by Viviani *et al.*⁴

The only advantage of the FHNC techniques compared with VMC is the possibility of analytic manipulation of the elements to calculate and a greater freedom in the choice of the correlating functions as they are not limited by the size of the simulation cube. Its main disadvantage is that we have to approximate the contribution of the elementary diagrams, important in the case of liquid ^3He . Moreover, we must remember that rough approximations must be done in FHNC equations if we want to use operational correlations and that there are no VMC calculations using full-spin-dependent correlations. So, independently of using FHNC or VMC, it would be desirable to exclude operational correlations in the wave function if possible. We must search for alternative mechanisms of correlations to operational correlations that avoid their difficulties.

As we have mentioned above, a partial option to full-spin correlations are correlations depending on the third component of spin, henceforth to be called σ_z -dependent correlations. The inclusion of these correlations does not modify too much the procedures used in the FHNC method for central two-body correlations. The increment of the bound energy provided by these correlations compared with central two-body correlations is about 0.2 K

at the experimental equilibrium density.⁹ This is 40% of the increment provided by full-spin correlations.⁴ On the other hand, the calculations with full-spin correlations have shown an important competition among these correlations, three-body, and specially backflow correlations.

$$\Psi(1,2,\dots,A) = \prod_{\substack{i,j=1 \\ i < j}}^A f(\mathbf{x}_i, \mathbf{x}_j) \prod_{\substack{i,j,k=1 \\ i < j < k}}^A f_3(r_{ij}, r_{ik}, r_{jk}) \prod_{\substack{i,j=1 \\ i < j}}^A e^{i\eta(r_{ij})\mathbf{r}_{ij}[\hat{K}(i) - \hat{K}(j)]} \Phi(1,2,\dots,A), \quad (1)$$

where $\Phi(1,2,\dots,A)$ is the Slater determinant that represents the noncorrelated Fermi sea, with a Fermi momentum $k_F = (6\pi\rho/\nu)^{1/3}$, ρ represents the density of the system, and ν is the degeneration of the spin states. The σ_z -dependent two-body correlation can be written as

$$f(\mathbf{x}_i, \mathbf{x}_j) = f_c(r_{ij}) + \sigma_z(i)\sigma_z(j)f_\sigma(r_{ij}). \quad (2)$$

The three-body correlation has the form

$$f_3(r_{ij}, r_{ik}, r_{jk}) = \exp \left[\frac{\lambda_r}{2} \sum_{\text{cyc}} \xi(r_{ij}) \xi(r_{ik}) \mathbf{r}_{ij} \cdot \mathbf{r}_{ik} \right], \quad (3)$$

where cyc represents a sum over the three terms obtained replacing ijk with jki and kij , and $\hat{K}(i)$ is an operator acting over $\Phi(1,2,\dots,A)$ as

$$\hat{K}(i) \exp \left[i \sum_{j=1}^A \mathbf{k}_{\alpha_j} \cdot \mathbf{r}_j \right] = \mathbf{k}_{\alpha_i} \exp \left[i \sum_{j=1}^A \mathbf{k}_{\alpha_j} \cdot \mathbf{r}_j \right]. \quad (4)$$

We shall use McMillan correlation for the central f_c part and the semioptimized function⁹ for the spin f_σ part of the σ_z -dependent correlation and the same parametrization as Manousakis *et al.*³ for the functions of the three-body $\xi(r)$ and backflow $\eta(r)$ correlations:

$$\xi(r) = e^{-[(r-r_i)/\omega_i]^2}, \quad (5)$$

$$\eta(r) = \lambda_b e^{-[(r-r_b)/\omega_b]^2}. \quad (6)$$

Apart from these choices, we shall use other parameterizations in order to compare with VMC calculations. So we shall use the forms of Schmidt *et al.*¹¹ for the three-body and backflow correlations. These can be obtained multiplying the previous functions by $[(r-R)/R]^3$ for $r < R$ and are equal to zero for $r > R$; this is essential for an adequate sampling in the VMC calculation.

II. FHNC EQUATIONS FOR THE TWO-BODY DISTRIBUTION FUNCTION

The calculation of the expectation value of the energy requires knowledge of the two- and three-body distribution functions related to the trial wave function proposed. These quantities can be calculated using the FHNC techniques. These techniques generate a set of integral and algebraic equations that involve different classes of diagrams. The distribution functions and the expectation value of any operator can be expressed in terms of these diagrams. The basic quantities needed to build the two- and three-body distributions already appear in the expansion of the two-body distribution function. Therefore we

One of the purposes of this work is to evaluate this behavior when we use σ_z -dependent correlations.

Our aim is to study the ground state of liquid ³He with a Jastrow trial wave function, which may be written as

shall pay special attention to this function, which is defined as

$$g(\mathbf{x}_1, \mathbf{x}_2) = \frac{A(A-1) \int |\Psi(\mathbf{x}_1, \dots, \mathbf{x}_A)|^2 d\mathbf{x}_3 \cdots d\mathbf{x}_A}{(\rho/\nu)^2 \int |\Psi(\mathbf{x}_1, \dots, \mathbf{x}_A)|^2 d\mathbf{x}_1 \cdots d\mathbf{x}_A}. \quad (7)$$

This function can be written in terms of the FHNC elements as

$$g(\mathbf{x}_1, \mathbf{x}_2) = g_{dd}(\mathbf{x}_1, \mathbf{x}_2) + g_{de}(\mathbf{x}_1, \mathbf{x}_2) + g_{ed}(\mathbf{x}_1, \mathbf{x}_2) + g_{ee}(\mathbf{x}_1, \mathbf{x}_2), \quad (8)$$

where $g_{mn}(\mathbf{x}_1, \mathbf{x}_2)$ are the different contributions to $g(\mathbf{x}_1, \mathbf{x}_2)$ with $mn = dd, de, ed, ee$, corresponding to diagrams with (e) or without (d) two statistical lines in particles 1 and 2, and \mathbf{x}_i represents the spatial and spin coordinates of the particle i . In order to build some of the ee diagrams, we must introduce some new quantities called cc diagrams. These are diagrams with only one statistical line in particles 1 and 2.

It is important to point out that if the backflow term is not included in the wave function, the construction of the FHNC equations is exact and there is no need of making any approximation, apart from the elementary diagrams. The noncommutation of backflow correlations makes the cluster expansion not irreducible,² and we have to do some approximations summing up only the simplest diagrams. We shall follow Manousakis *et al.*³ in this case.

The FHNC equations were first obtained by Fantoni and Rosati⁵ for central two-body correlations. After this, these equations were generalized by Schmidt and Pandharipande² in order to include three-body correlations. The inclusion of σ_z -depend correlations does not modify drastically the FHNC equations in both cases. The first one was studied by Kürten and Campbell.¹³ The generalization to include three-body correlations is quite straightforward, following the same line as the two-body case, and it will not be discussed here.

In order to calculate the kinetic energy, it is necessary to know not only the two- but also the three-body distribution functions. Almost all the diagrammatic elements needed to build this distribution function are present in the two-body distribution function. We have to add the so-called Abe diagrams¹⁴ A_{mnl} , which are diagrams with three external points. In all the previous calculations, only A_{ddd} has been taken into account. We shall use the same approximation, and then the three-body distribution function $g_3(\mathbf{x}_1, \mathbf{x}_2, \mathbf{x}_3)$ can be written as

$$g_3(\mathbf{x}_1, \mathbf{x}_2, \mathbf{x}_3) = f_3^2(r_{12}, r_{13}, r_{23}) [1 + A_{ddd}(\mathbf{x}_1, \mathbf{x}_2, \mathbf{x}_3)] \times \left[\sum_{l'm'm'n'} \vartheta_{l'l'} \vartheta_{mm'} \vartheta_{nn'} g_{lm}(\mathbf{x}_1, \mathbf{x}_2) g_{l'n}(\mathbf{x}_1, \mathbf{x}_3) g_{m'n'}(\mathbf{x}_2, \mathbf{x}_3) - 2g_{cc}(\mathbf{x}_1, \mathbf{x}_2) g_{cc}(\mathbf{x}_1, \mathbf{x}_3) g_{cc}(\mathbf{x}_2, \mathbf{x}_3) \right], \quad (9)$$

where $l(l'), m(m'), n(n') = d, e$ and

$$\vartheta_{ll'} = \delta_{ll', dd} + \delta_{ll', de} + \delta_{ll', ee}. \quad (10)$$

$\delta_{ll', nm}$ is 1 or 0 if $ll' = mn$, or not. We must note that all the quantities built depend on the spatial coordinates of the particles and on their third component of spin. This last fact obliges us to decompose the functions for calculations.¹³ This may be done in two different ways. The first one separates the part without spin dependence, called the central part, from that with spin dependence, known as the spin part. This is

$$A(\mathbf{x}_i, \mathbf{x}_j) = A_c(r_{ij}) + A_\sigma(r_{ij}) \sigma_z(i) \sigma_z(j). \quad (11)$$

The second one separates the contribution of particles with parallel third components of spin, the parallel part, from the contribution of particles with antiparallel third components of spin, the antiparallel part:

$$A(\mathbf{x}_i, \mathbf{x}_j) = A_p(r_{ij}) P_p(ij) + A_a(r_{ij}) P_a(ij), \quad (12)$$

where we have written P_p and P_a for the projectors over states with parallel and antiparallel third components of spin. This is

$$Z(\mathbf{x}_1, \mathbf{x}_2) = \frac{2\rho}{v r_{12}} \sum_{l,l'} \vartheta_{ll'} \int d\mathbf{x}_3 \hat{\mathbf{r}}_{12} \cdot \hat{\mathbf{r}}_{13} r_{13} \eta(r_{13}) f_3^2(r_{12}, r_{13}, r_{23}) g_{dl}(\mathbf{x}_1, \mathbf{x}_3) g_{dl'}(\mathbf{x}_2, \mathbf{x}_3). \quad (15)$$

Apart from the modification of the Slater function, the backflow correlations generate new diagrams which must be included.³

The FHNC method does not provide a way for summing up all the elementary and Abe diagrams. Then we shall have to use different approximations for these kinds of diagrams. In our calculation we have used and extended both the scaling approximation FHNC/s (Refs. 3 and 6) and the interpolating equation approximation FHNC/ $\alpha(r)$.⁷

The first one has been applied following the same scheme as Manousakis *et al.*,³ neglecting the elementary diagrams caused by the spin and backflow correlations and only including the elementary diagrams produced by central two- and three-body correlations. The free parameter, the scaling constant s , is fixed, equating the kinetic energy calculated using the Jackson-Feenberg form¹⁶ with the Pandharipande-Bethe form¹⁷ only when central two-body correlations are included.

In the case of the interpolating equation approximation, we have generalized the equations obtained for two-body central and σ_z -dependent correlations.⁹ Backflow elementary diagrams are neglected, but the

$$P_p(ij) = \frac{1 + \sigma_z(i) \sigma_z(j)}{2}, \quad (13)$$

$$P_a(ij) = \frac{1 - \sigma_z(i) \sigma_z(j)}{2}.$$

It must be noted that A_μ , $\mu = c, \sigma, p, a$, depends only on the distance between the particles. The three-body distribution function and an Abe diagram can be decomposed in a similar way.

The inclusion of backflow correlations in the wave function complicates the diagrammatic analysis for the two-body distribution function. The approximation used by Schmidt and Pandharipande² includes only the two- and three-body clusters. This is a crude approximation, but it looks adequate for calculating with these correlations.^{3,4} The extension of this approximation for σ_z -dependent correlations is quite straightforward and the modifications parallel to those performed for two- and three-body correlations. The most important effect of backflow is to modify the argument of the Slater function $l(k_F r_{ij})$, which is a *cc* diagram, to

$$\mathcal{L}(k_F r_{ij}) = l(k_F t(r_{ij})) = l(k_F r_{ij} [1 + 2\eta(r_{ij}) + Z_p(r_{ij})]), \quad (14)$$

where Z_p is the parallel part of

influence of the spin correlations is included using approximation II described in Ref. 9. The three-body elementary diagrams are included using the extensions described in Refs. 4 and 12. We must remember that apart from the interpolating parameter, which is fixed using the bosonic system in this last case, we must use a scaling constant for the Abe diagrams that is fixed in the same ways as that for the scaling approximation. In this case this constant does not scale the elementary diagrams.

III. EXPECTATION VALUE OF THE HAMILTONIAN

The Hamiltonian which describes the system of A atoms of ${}^3\text{He}$ is quite simple because the interaction depends only on the relative distance among the particles. Then

$$H(1, \dots, A) = -\frac{\hbar^2}{2m} \sum_{i=1}^A \nabla_i^2 + \sum_{\substack{i,j=1 \\ i < j}}^A V(r_{ij}). \quad (16)$$

We shall use as interaction the HFDHE2 potential of Aziz *et al.*,¹⁵ which is the best parametrization of the in-

teraction between two helium atoms. Moreover, there is strong evidence that it is close to the exact one.^{1,4}

The expectation value of the Hamiltonian per particle may be divided in two parts corresponding to the potential and kinetic energies. The first one is easily expressed in terms of the two-body distribution function

$$\langle V \rangle / A = \frac{\rho^2}{v^2 2 A} \int d\mathbf{x}_1 d\mathbf{x}_2 V(r_{12}) g(\mathbf{x}_1, \mathbf{x}_2). \quad (17)$$

The expectation value of the kinetic energy is not so straightforward as the last one because the action of the Laplacian modifies the elements in the wave function. This forces the generation of new diagrammatic elements to describe these modifications. On the other hand, there are different forms of calculating the kinetic energy depending on whether the Laplacian acts over the "bra" or "ket." Obviously, any of the options would supply the

same value for an exact calculation, but as we must do approximations, the values may be different. This fact is used for fixing the scaling constant of the elementary and Abe diagrams in the scaling approximation, as we have already mentioned.

There are three options that are the most used for the calculation of the kinetic energy per particle. They are the Jackson-Feenberg,¹⁶ Pandharipande-Bethe,¹⁷ and Clark-Westhaus¹⁸ forms. The last two forms are useful only for two-body correlations, because for three-body correlations they both depend on the four- and five-body distribution functions.¹⁹ The expression for these form when only central two-body correlations are present can be found in Ref. 6 and can be easily generalized for σ_z -dependent correlations.

We shall analyze the Jackson-Feenberg form. This can be written in a general case as

$$\begin{aligned} T_{\text{JF}} = \frac{-\hbar^2}{4m A \langle \Psi | \Psi \rangle} \sum_{i=1}^A \int d\mathbf{x}_1 \cdots d\mathbf{x}_A \{ & (\nabla_i^\dagger \Phi^*) F^\dagger F \Phi + \Phi^* F^\dagger F (\nabla_i^2 \Phi) + (\nabla_i \Phi^*) \cdot [(\nabla_i F^\dagger) F - F^\dagger (\nabla_i F)] \Phi \\ & + \Phi^* [F^\dagger (\nabla_i F) - (\nabla_i F^\dagger) F] \cdot (\nabla_i \Phi) - \frac{1}{2} \nabla_{i,\Phi}^2 (\Phi^* F^\dagger F \Phi) \\ & + \frac{1}{2} \Phi^* [(\nabla_i^2 F^\dagger) F + F^\dagger (\nabla_i^2 F) - 2(\nabla_i F^\dagger) \cdot (\nabla_i F)] \Phi \}, \end{aligned} \quad (18)$$

where we have supposed that the correlating factor F is not self-adjoint, this being only necessary if we include backflow correlations, and $\nabla_{i,\Phi}$ means that the gradients only act over Φ and Φ^* .

The two first terms correspond to the energy per particle of the Fermi gas $T_F = 3\hbar^2 k_F^2 / 10m$. The third and the fourth terms only are different from zero when backflow correlations are present. If three-body parts are neglected, this can be written as

$$T_K = \frac{\hbar^2 k_F^2 \rho^2}{5m A v^2} \int d\mathbf{x}_1 d\mathbf{x}_2 [r_{12} \eta'(r_{12}) + 3\eta(r_{12})] [g_{dd}(\mathbf{x}_1, \mathbf{x}_2) + g_{de}(\mathbf{x}_1, \mathbf{x}_2)]. \quad (19)$$

The fifth term has two- and three-body contributions, but this last one can be neglected, and so we can write

$$\begin{aligned} W_\phi = \frac{\hbar^2 \rho^2}{4m A v^2} \int d\mathbf{x}_1 d\mathbf{x}_2 \{ & g_{cc}(\mathbf{x}_1, \mathbf{x}_2) \nabla_{i(r_{12})}^2 \mathcal{L}(k_F r_{12}) \delta_{\sigma_z(1)\sigma_z(2)} \\ & - g_{dd}(\mathbf{x}_1, \mathbf{x}_2) [\mathcal{L}'(k_F r_{12}) \delta_{\sigma_z(1)\sigma_z(2)}]^2 - N_{cc}(\mathbf{x}_1, \mathbf{x}_2) \nabla_i^2 l(k_F r_{12}) \delta_{\sigma_z(1)\sigma_z(2)} \}, \end{aligned} \quad (20)$$

where

$$\mathcal{L}'(k_F r_{ij}) = \frac{\partial l[k_F t(r_{ij})]}{\partial t(r_{ij})}. \quad (21)$$

The last term is the only term that will hold for a bosonic fluid and, if three-body backflow terms are neglected, is

$$\begin{aligned} T_B = \frac{-\hbar^2 \rho^2}{4m A v^2} \int d\mathbf{x}_1 d\mathbf{x}_2 g^*(\mathbf{x}_1, \mathbf{x}_2) \{ & f(\mathbf{x}_1, \mathbf{x}_2) \nabla_1^2 f(\mathbf{x}_1, \mathbf{x}_2) - [\nabla_1 f(\mathbf{x}_1, \mathbf{x}_2)]^2 \} \\ & \times \frac{-\hbar^2 \rho^3}{8m A v^3} \int d\mathbf{x}_1 d\mathbf{x}_2 d\mathbf{x}_3 g_3^*(\mathbf{x}_1, \mathbf{x}_2, \mathbf{x}_3) \{ f_3(r_{12}, r_{13}, r_{23}) \nabla_1^2 f_3(r_{12}, r_{13}, r_{23}) - [\nabla_1 f_3(r_{12}, r_{13}, r_{23})]^2 \} \\ & \times \frac{-\hbar^2 \rho^2}{2m A v^2} \int d\mathbf{x}_1 d\mathbf{x}_2 [r_{12} \eta''(r_{12}) + 4\eta'(r_{12})] g_{cc}(\mathbf{x}_1, \mathbf{x}_2) \mathcal{L}'(k_F r_{12}) \delta_{\sigma_z(1)\sigma_z(2)} \\ & + \frac{\hbar^2 k_F^2 \rho^2}{5m A v^2} \int d\mathbf{x}_1 d\mathbf{x}_2 \{ [r_{12} \eta'(r_{12}) + \eta(r_{12})]^2 + 2\eta^2(r_{12}) \} [g_{dd}(\mathbf{x}_1, \mathbf{x}_2) + g_{de}(\mathbf{x}_1, \mathbf{x}_2)], \end{aligned} \quad (22)$$

where we have defined

$$g(\mathbf{x}_1, \mathbf{x}_2) = f^2(\mathbf{x}_1, \mathbf{x}_2)g^*(\mathbf{x}_1, \mathbf{x}_2),$$

$$g_3(\mathbf{x}_1, \mathbf{x}_2, \mathbf{x}_3) = f_3^2(r_{12}, r_{13}, r_{23})g_3^*(\mathbf{x}_1, \mathbf{x}_2, \mathbf{x}_3).$$

IV. RESULTS

The factorized structure of our trial wave function (1) makes it possible to introduce the different mechanisms of correlation independently. This allows us to study their mutual influence and competition separately. Because of the approximations performed with backflow correlations and the elementary and Abe diagrams, it is necessary to establish their validity. The approximations used here are not new and have been compared with VMC calculations of the energy per particle with functions that include central two- and three-body correlations and backflow correlations¹¹ and with functions that include only central two-body and σ_z -dependent correlations.¹⁰ These VMC results are in good agreement with those provided by FHNC/ $\alpha(r)$ (Ref. 4) and FHNC/ s (Ref. 6) for densities around the experimental equilibrium density. In Table I we compare our results at $\rho = 0.237\sigma^{-3}$ using both approximations with the VMC calculations of Schmidt *et al.*¹¹ For higher densities^{4,3} the agreement worsens slightly when three-body and backflow are introduced. It must be noted that the most important differences appear when backflow correlations are included.

However, we must keep in mind that VMC calculations cannot be carried for any correlation function because the range of the correlations must be limited by the size of the box where the sampling is performed. This limitation disappears when we use FHNC method and allows a better optimization of the whole wave function. The change of the correlation functions makes the test with VMC calculations not possible. So the only possible test is to compare the FHNC/ $\alpha(r)$ results with the FHNC/ s ones because the elementary diagrams are generated in two different ways. On the other hand, as we are mainly interested in the role of σ_z -dependent correla-

TABLE I. Comparison of our results with the VMC results from Ref. 11. In this case the σ_z -dependent correlations are not present. J (Jastrow) is written when central two-body correlations are included, T (triplet) when three-body are present, and B (backflow) when these correlations are in the wave function. The calculation is at $\rho = 0.237\sigma^{-3}$ and with use of the Aziz potential. For more details in the wave function, see Ref. 11.

		V	E	E (VMC)
J	FHNC/ s	-11.99	-1.36	-1.38±0.02
	FHNC/ $\alpha(r)$	-12.02	-1.38	
$J + T$	FHNC/ s	-12.01	-1.66	-1.68±0.02
	FHNC/ $\alpha(r)$	-12.03	-1.65	
$J + T + B$	FHNC/ s	-11.84	-1.89	-1.99±0.02
	FHNC/ $\alpha(r)$	-11.86	-1.92	

tions, we shall keep the central two-body function in the McMillan²⁰ form. This correlation function does not include long-range effects, but this omission has an effect only on the total bound energy and it is independent of the correlation mechanisms included. In order to include long-range correlations, it is also necessary to change the criterion for fixing the interpolating constant.²¹ All these facts and the possibility of comparing with VMC calculations have led us to use McMillan correlation. As we have already mentioned, we have used for the three-body and backflow correlations the form and values of the parameters from Usmani, Fantoni, and Pandharipande.¹⁹ This choice allows an indirect comparison with their results⁶ because the difference between the energies will be caused by the inclusion in their calculations of long-range central two-body correlations. For the spin part of the σ_z -dependent correlation, we have solved the variational problem for this correlation function when all the central diagrams have been included, but only the two-body diagrams for the spin part. This is a generalization of the spin part obtained when we only use two-body correlations.⁹ The equations are listed in the Appendix. The results for these wave functions are collected in Table II for FHNC/ s and FHNC/ $\alpha(r)$ and using the Aziz potential.

The most remarkable thing in the results is the good agreement between the results provided by the two approximation used. This agreement is maintained for the potential and kinetic energies. It is also remarkable that the comparison without σ_z -dependent correlations compare well with those of Manousakis *et al.*³ and Viviani *et al.*,⁴ and the differences are caused because they use optimized central two-body correlations that include long-range effects. These differences remain almost constant when the other mechanisms of correlation are taken into account.

The inclusion of the dependence of spin introduces an

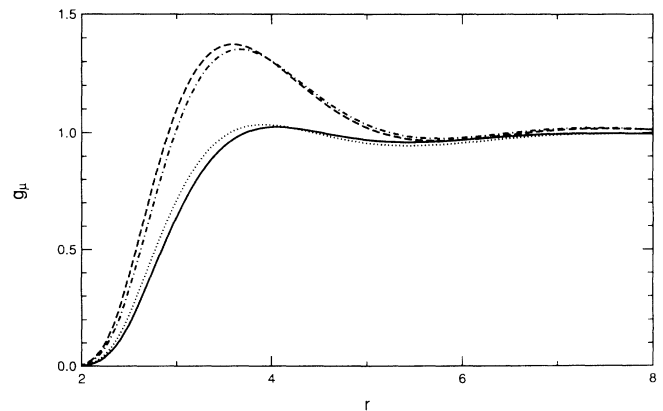


FIG. 1. Dotted and solid lines are the parallel parts of the two-body distribution function with and without σ_z -dependent correlations, respectively. Dot-dashed and dashed lines are the antiparallel parts of the two-body distribution function with and without σ_z -dependent correlations, respectively. These functions correspond to a calculation with central two- and three-body correlations using an interpolating approximation at $\rho = 0.277\sigma^{-3}$. The energies can be seen in Table II.

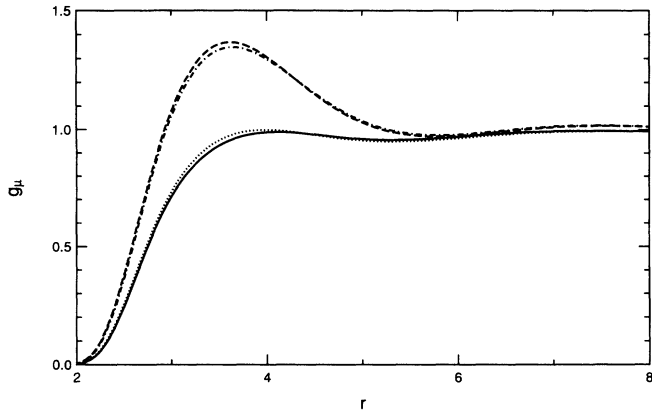


FIG. 2. Same as Fig. 1, but backflow correlations are also included in this case.

increment of the bound energy between 0.1 and 0.15, increasing slightly for higher densities when backflow correlations are not present. When backflow correlations are present, the inclusion of σ_z -dependent correlations does not supply any appreciable increment of the bound energy for all the densities studied. The graphics of the parallel and antiparallel parts of the two-body correlation functions shown in Figs. 1 and 2 can clarify something about the competition between σ_z -dependent and backflow correlations. Figure 1 shows the results for central two- and three-body correlations compared with the case when σ_z -dependent correlations are also included.

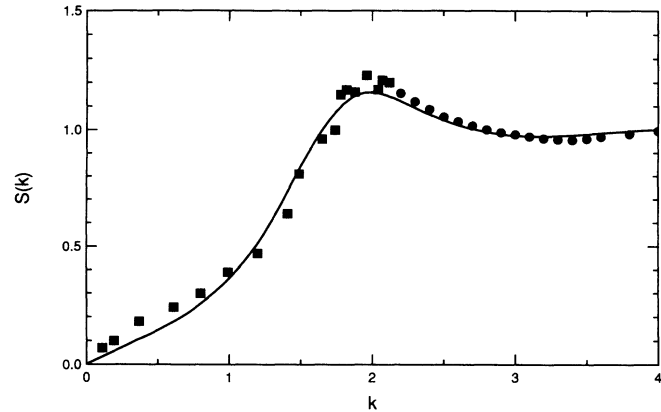


FIG. 3. Structure function obtained in a calculation with all the mechanisms of correlation included is compared with the experimental data at the equilibrium density. Squares are data from Ref. 24 at $T=0.41$ K, and circles are from Ref. 23 at $T=0.56$ K.

We watch a displacement to the right in the parallel channel and to the left in the antiparallel channel when σ_z -dependent correlations are introduced. Moreover, the parallel component increases and the antiparallel decreases around the first maximum when σ_z -dependent correlations are present. We must stress that the central part is not modified. In Fig. 2 we represent the same quantities those in Fig. 1, but when backflow correlations

TABLE II. Calculation with scaling (FHNC/s) and interpolating equation [FHNC/ $\alpha(r)$] approximation. We use the same notation that in Table I. We use $f_\sigma \neq 0$ to say that σ_z -dependent correlations are present.

$\rho(\sigma^{-3})$		$f_\sigma = 0$				$f_\sigma \neq 0$			
		FHNC/ $\alpha(r)$		FHNC/s		FHNC/ $\alpha(r)$		FHNC/s	
		V	E	V	E	V	E	V	E
0.200	J	-9.83	-1.36	-9.80	-1.33	-9.87	-1.42	-9.84	-1.40
	J+B	-9.77	-1.69	-9.75	-1.69	-9.76	-1.70	-9.74	-1.70
	J+T	-9.84	-1.56	-9.81	-1.54	-9.88	-1.62	-9.85	-1.59
	J+T+B	-9.78	-1.89	-9.76	-1.87	-9.78	-1.91	-9.76	-1.89
0.237	J	-12.02	-1.38	-11.99	-1.36	-12.10	-1.47	-12.08	-1.44
	J+B	-11.92	-1.79	-11.90	-1.79	-11.92	-1.81	-11.91	-1.81
	J+T	-12.06	-1.75	-12.03	-1.73	-12.13	-1.82	-12.11	-1.80
	J+T+B	-11.95	-2.15	-11.93	-2.13	-11.96	-2.16	-11.94	-2.14
0.277	J	-14.34	-1.10	-14.32	-1.08	-14.45	-1.21	-14.45	-1.19
	J+B	-14.16	-1.57	-14.16	-1.59	-14.18	-1.59	-14.18	-1.60
	J+T	-14.39	-1.70	-14.38	-1.69	-14.50	-1.79	-14.49	-1.78
	J+T+B	-14.21	-2.15	-14.19	-2.14	-14.22	-2.16	-14.22	-2.15
0.300	J	-15.61	-0.75	-15.61	-0.75	-15.76	-0.88	-15.77	-0.88
	J+B	-15.39	-1.26	-15.41	-1.30	-15.41	-1.28	-15.44	-1.32
	J+T	-15.66	-1.50	-15.67	-1.52	-15.80	-1.60	-15.81	-1.62
	J+T+B	-15.42	-1.98	-15.42	-1.97	-15.45	-1.99	-15.46	-1.99
0.330	J	-17.17	-0.06	-17.22	-0.13	-17.36	-0.22	-17.42	-0.27
	J+B	-16.89	-0.61	-16.96	-0.71	-16.93	-0.63	-17.01	-0.72
	J+T	-17.19	-1.00	-17.25	-1.08	-17.36	-1.13	-17.43	-1.20
	J+T+B	-16.87	-1.50	-16.90	-1.54	-16.91	-1.51	-16.96	-1.55
0.360	J	-18.58	0.93	-18.74	0.73	-18.81	0.76	-18.97	0.57
	J+B	-18.24	0.36	-18.41	0.13	-18.29	0.33	-18.47	0.11
	J+T	-18.50	-0.15	-18.66	-0.36	-18.71	-0.31	-18.87	-0.50
	J+T+B	-18.09	-0.65	-18.21	-0.78	-17.96	-0.65	-18.28	-0.81

TABLE III. Position of the equilibrium density (ρ_0) and energy (E_0), sound velocity (c), and compressibility (κ) at this equilibrium density for the different kinds of correlations employed in the work. We use the same notation that in Tables I and II. All these quantities are almost independent of the approximation for the elementary diagrams used.

		ρ_0 (σ^{-3})	E_0 (K)	c (m/s)	κ (atm^{-1})
J	$f_\sigma=0$	0.221	-1.40	153.0	0.052
	$f_\sigma \neq 0$	0.226	-1.48	159.0	0.048
$J+B$	$f_\sigma=0$	0.232	-1.79	170.0	0.042
	$f_\sigma \neq 0$	0.232	-1.80	170.0	0.042
$J+T$	$f_\sigma=0$	0.251	-1.79	192.0	0.033
	$f_\sigma \neq 0$	0.253	-1.86	193.0	0.033
$J+T+B$	$f_\sigma=0$	0.258	-2.15	207.0	0.028
	$f_\sigma \neq 0$	0.258	-2.16	207.0	0.028

are also present now. The fundamental difference between both figures is that the displacement observed in Fig. 1 disappears in Fig. 2. This indicates that a similar displacement is caused by backflow, and it generates the increase in the bound energy due to σ_z -dependent correlations in the other cases. Finally, we must also point out that this behavior is maintained when the three-body correlations are not included in the calculations and that the only difference in the parts of the distribution function when three-body correlations are present is a small displacement in the first maximum to greater relative distances.

Another important aspect to be studied is the behavior of the energy per particle as a function of the density and especially the position of the minimum when the different mechanisms are included. The results are similar to those obtained in other works and are collected in Table III. The inclusion of triplet correlations moves appreciably the minimum to higher densities compared with when only central two-body correlations are present. The backflow correlation generates the same effect, but quite smaller compared with triplet correlations. The effect of σ_z -dependent correlations is very small and does not modify the position of the minimum. In Table III we have also calculated the sound velocity and compressibility in every case. The agreement with the experimental sound velocity 182.90 m/s (Ref. 22) is reasonable.

Figure 3 shows the structure function $S(k)$, which is the Fourier transform of the central part of the two-body correlation function when all the correlations are included and compared with the experimental data.^{23,24} It is evident that the agreement is not good for small momenta because the long-range behavior is not included in our wave functions. However, the agreement improves for higher momenta.

V. CONCLUSIONS

We must emphasize two aspects in this work. The first one is the attention given to the approximation of the ele-

mentary diagrams, which is one of the most important problems in this kind of calculation. We must stress the good resemblance of the results in all the studied cases between the FHNC/ s and FHNC/ $\alpha(r)$, not only for the total energy, but also for the kinetic and potential energies. Nevertheless, this agreement worsens when the density increases. It is also important to point out that this is the first time that both approximations have been applied using the same programs.

The second and most important aspect is how backflow correlations absorb the increment of the energy provided by σ_z -dependent correlations, although this increment had not been modified by the inclusion of three-body correlations. This shows that the effect introduced by σ_z -dependent correlations is already present in the backflow correlations. However, as it can be seen in Fig. 2, the inclusion of σ_z -dependent correlations modifies the form of the two-body distribution function even when the backflow is present. We must remember that this kind of competition is also watched when full-spin correlations are used.⁴

APPENDIX

Here we give the equations obtained from the process of minimization for the spin part of the correlation function following the process described in Ref. 9 when backflow correlations are included. We shall use the same notation as Ref. 9, which must be consulted for further explanations.

The spin part of the correlation $f_\sigma(r)$ is the solution of the differential equation

$$y'' + \left[G_1 - \frac{\lambda}{2g_c^*} \right] y + G_2 = 0, \quad (\text{A1})$$

with the contour conditions

$$f_\sigma(0) = f_\sigma(d_\sigma) = f'_\sigma(d_\sigma) = 0, \quad (\text{A2})$$

where d_σ is a variational parameter and

$$y = r(g_c^*)^{1/2} f_\sigma, \quad (\text{A3})$$

$$\begin{aligned}
G_1 = & -\frac{m}{\hbar^2} V - \frac{\nabla^2 g_c^*}{4g_c^*} + \left[\frac{\nabla g_c^*}{2g_c^*} \right]^2 + \frac{1}{2g_c^*} \exp(N_{dd}^c + E_{dd}^c) [(\mathcal{L}')^2 / \nu - (\nabla_i^2 \mathcal{L})(N_{cc}^c + D_{cc}^c + E_{cc}^c - \mathcal{L} / \nu)] \\
& + \frac{1}{g_c^*} \exp(N_{dd}^c + E_{dd}^c) (N_{cc}^c + D_{cc}^c + E_{cc}^c - \mathcal{L} / \nu) \mathcal{L}' (r\eta'' + 4\eta') \\
& - \frac{2k_F^2}{5g_c^*} \exp(N_{dd}^c + E_{dd}^c) (1 + N_{de}^c + E_{de}^c + D_{de}^c) [(r\eta)^2 + 2r\eta\eta' + 3\eta^2 + r\eta' + 3\eta] , \\
G_2 = & \frac{r}{(g_c^*)^{1/2}} \left[-\frac{m}{\hbar^2} V f_c g_\sigma^* + g_\sigma^* \nabla^2 f_c + \nabla f_c \nabla g_\sigma^* + \frac{1}{4} f_c \nabla^2 g_\sigma^* \right. \\
& + \frac{1}{2} f_c \exp(N_{dd}^c + E_{dd}^c) [(\mathcal{L}')^2 / \nu - (\nabla_i^2 \mathcal{L})(N_{cc}^c + D_{cc}^c + E_{cc}^c - \mathcal{L} / \nu)] \\
& \left. + f_c \exp(N_{dd}^c + E_{dd}^c) (N_{cc}^c + D_{cc}^c + E_{cc}^c - \mathcal{L} / \nu) \mathcal{L}' (r\eta'' + 4\eta') \right] , \\
g_c^* = & \exp(N_{dd}^c + E_{dd}^c) [(1 + N_{de}^c + E_{de}^c + D_{de}^c)^2 + N_{ee}^c + E_{ee}^c + D_{ee}^c - \nu(N_{cc}^c + E_{cc}^c + D_{cc}^c - \mathcal{L} / \nu)^2] , \\
g_\sigma^* = & \exp(N_{dd}^c + E_{dd}^c) [D_{ee}^{(2)c} - \nu(N_{cc}^c + E_{cc}^c + D_{cc}^c - \mathcal{L} / \nu)^2] .
\end{aligned} \tag{A4}$$

- ¹R. M. Panoff and J. Carlson, Phys. Rev. Lett. **62**, 1130 (1989).
²K. E. Schmidt and V. R. Pandharipande, Phys. Rev. B **19**, 2504 (1979).
³E. Manousakis, S. Fantoni, V. R. Pandharipande, and Q. N. Usmani, Phys. Rev. B **28**, 3770 (1983).
⁴M. Viviani, E. Buendía, S. Fantoni, and S. Rosati, Phys. Rev. B **38**, 4523 (1988).
⁵S. Fantoni and S. Rosati, Nuovo Cimento A **25**, 593 (1975).
⁶Q. N. Usmani, B. Friedman, and V. R. Pandharipande, Phys. Rev. B **25**, 4502 (1982).
⁷A. Fabrocini and S. Rosati, Nuovo Cimento D **1**, 567 (1982).
⁸A. Fabrocini and S. Rosati, Nuovo Cimento D **1**, 615 (1982).
⁹F. Arias de Saavedra and E. Buendía, Phys. Rev. B **42**, 6018 (1989).
¹⁰K. E. Kürten and J. W. Clark, Phys. Rev. B **30**, 1342 (1984).
¹¹K. E. Schmidt, M. A. Lee, M. H. Kalos, and G. V. Chester, Phys. Rev. Lett. **47**, 807 (1981).
¹²S. Rosati, E. Buendía, and M. Viviani (unpublished).

- ¹³K. E. Kürten and C. E. Campbell, J. Low Temp. Phys. **44**, 149 (1981).
¹⁴R. Abe, Prog. Theor. Phys. **21**, 421 (1959).
¹⁵R. A. Aziz, P. S. Nain, J. S. Carley, W. L. Taylor, and G. T. Conville, J. Chem. Phys. **70**, 4330 (1979).
¹⁶H. W. Jackson and E. Feenberg, Ann. Phys. (N.Y.) **15**, 266 (1961).
¹⁷V. R. Pandharipande and H. A. Bethe, Phys. Rev. C **7**, 1312 (1973).
¹⁸J. W. Clark and P. Westhaus, J. Math. Phys. **9**, 131 (1968).
¹⁹Q. N. Usmani, S. Fantoni, and V. R. Pandharipande, Phys. Rev. B **26**, 6123 (1982).
²⁰W. L. McMillan, Phys. Rev. **138**, 442 (1965).
²¹M. Viviani, E. Buendía, A. Fabrocini, and S. Rosati, Nuovo Cimento D **8**, 561 (1986).
²²R. A. Aziz and R. K. Pathria, Phys. Rev. A **7**, 809 (1973).
²³E. K. Achter and L. Meyer, Phys. Rev. **188**, 51 (1969).
²⁴R. B. Hallock, J. Low Temp. Phys. **9**, 109 (1972).